Nanoscale Horizons

ROYAL SOCIETY OF CHEMISTRY

COMMUNICATION

View Article Online
View Journal

Check for updates

Cite this: DOI: 10.1039/d5nh00388a

Received 1st June 2025,
Accepted 24th July 2025

DOI: 10.1039/d5nh00388a

rsc.li/nanoscale-horizons

Published on 25 2025. Downloaded on 08.08.2025 20:24:34.

High-efficiency gold recovery from electronic waste with 2D silicon nanosheets†

Dingxuan Kang,‡[a] Chuanwang Xing,‡[a] Chengcheng Zhang,[a] Shenghua Wang,[a] Yuhang Dong,[a] Deren Yang [a] and Wei Sun *[ab]

Electronic waste (e-waste) has become one of the fastest-growing solid waste streams globally, with most e-waste containing significant quantities of high-value yet environmentally hazardous substances, particularly noble metals exemplified by gold (Au). These elements not only pose a potential threat to the environment and human health but also carry substantial economic value. Thus, the efficient and eco-friendly recovery of noble metals from e-waste can simultaneously mitigate environmental pollution and generate significant economic benefits. In this work, silicon—the second most abundant and cost-effective element in the Earth's crust—was utilized to synthesize two-dimensional silicon nanosheets (SiNSs) capable of highly efficient gold ion extraction. The SiNSs demonstrated exceptional extraction capacities (as high as 1500 mg Au per gram of SiNSs) at low concentrations (10 ppm). The redox-mediated mechanism governing Au extraction exhibited a lower energy barrier than traditional chemisorption. Furthermore, a continuous-flow extraction device was engineered, in which SiNS membranes maintained remarkable extraction performance even for ultralow-concentration Au ions (100 ppb).

New concepts

We report a cost-effective, two-dimensional silicon (an earth-abundant element) nanosheet (2D SiNS) platform for gold ion extraction from e-waste solutions. Unlike conventional adsorbents that rely on adsorption-based mechanisms, our system operates *via* a redox-mediated extraction process, exhibiting significantly lower energy barriers compared to traditional adsorption methods. In contrast to most studies conducted at high gold ion concentrations (>100 ppm), the developed SiNS platform demonstrates exceptional extraction capability in both low-concentration (10 ppm) and ultradilute (10 ppb) Au^{3+} solutions. To better simulate industrial-scale gold recovery scenarios, we designed a continuous-flow extraction system, surpassing conventional batch mixing approaches; this system achieves remarkable performance even at ultralow concentrations (100 ppb). Furthermore, this work validates the practical applicability of SiNSs using real-world e-waste leachates containing gold recovered from discarded CPUs. We demonstrate that this methodology establishes an efficient and economically viable strategy for electronic wastewater treatment and precious metal recovery, positioning 2D silicon materials as a highly promising class of materials for sustainable e-waste recycling processes.

Introduction

With the rapid advancement of electronic technology, electronic waste (e-waste) has become the fastest growing solid waste in the world. According to a report from the United Nations Environment Program (UNEP), the global e-waste production was 53.6 million tons in 2019 and is expected to reach 74.7 million tons by 2030. E-waste contains a large amount of hazardous substances such as organic matter and metal ions. The most valuable components in e-waste are the precious metals, such as gold (Au), silver (Ag), and palladium (Pd). Particularly, Au accounts for the highest value in e-waste, with a huge estimated consumption of over 300 tonnes per year.[1,2] The data from the International Resource Group (IRG) indicate

Wei Sun

As a longtime researcher in nano-silicon applications spanning catalysis, environmental remediation, and novel devices, I have been an avid reader of Nanoscale Horizons due to the exceptional alignment between my work and the journal's scope. While previously publishing in sister RSC journals, contributing my first article here—especially to this landmark 10th-anniversary collection—is a profound honour and career highlight. Congratulations to Nanoscale Horizons on a decade of groundbreaking research that has profoundly shaped our field.

[a] State Key Laboratory of Silicon and Advanced Semiconductor Materials, School of Materials Science and Engineering, Zhejiang University, Hangzhou 310027, China. E-mail: sunnyway423@zju.edu.cn

[b] Shangyu Institute of Semiconductor Materials, Zhejiang University, Shaoxing 312399, China

† Electronic supplementary information (ESI) available. See DOI: https://doi.org/10.1039/d5nh00388a

‡ These authors contributed equally to this work.

Published on 25 2025. Downloaded on 08.08.2025 20:24:34.

that the value of precious metal elements contained in global e-waste in 2019 was approximately $57 billion. This number even exceeds the gross domestic product (GDP) of most countries. Therefore, the efficient recovery of precious metal elements from e-waste is essential for the sustainable use of precious metal resources and eco-friendly e-waste recycling.

Among the various recovery methods for Au, hydrometallurgical techniques have been intensively researched in recent decades, due to their affordability, higher predictability, and lower environmental impact.[1,3] In such strategies, after an initial leaching process to extract metal ions from the e-waste solid into a solution resembling gold-containing wastewater, multiple steps are often necessary for further concentration/isolation of the ions (*e.g. via* adsorption, ion exchange, and solvent extraction), and the final recovery of Au in the metallic state *via* reductive means (*e.g. via* the electrorefining process, chemical reduction, and crystallization).[3] Solid materials are frequently utilized in these follow-up steps and significant progress has been achieved particularly for adsorption and reduction, but real-world e-waste recycling remains challenging. For example, the widely used traditional adsorbent activated carbon has shown relatively low adsorption capacity, slow adsorption kinetics, and poor selectivity, and it cannot reduce precious metal elements into their metallic state. Meanwhile, most of the emerging materials only showed high gold extraction capacity at relatively high gold concentrations of 500–3000 ppm.[4–10] However, within the gold concentration range of real-world e-waste recycling (from ppb levels to tens of ppm),[4,5,11] their extraction capacities typically decrease to below 250 mg g^{-1}. Besides, the reduction/cementation process (*e.g.* using Zn dust, Fe, *etc.*) to reduce Au often involves cyanide complexes and has stringent requirement on pH.[2] Besides, the selectivity to gold against other metal elements from real electronics,[12,13] and the economic viability of the material consumed for recovering gold also need further optimization. Therefore, researchers have always been exploring novel and economic materials for selectively recovering the diluted precious metal ions from the complex leached solutions.[1,5,14,15]

In recent years, two-dimensional (2D) materials have gained significant attention and have become a focal point of scientific research. Due to their high specific surface area, catalytic activity, chemical stability, and easy preparation, they demonstrate significant potential for recovering and loading precious metal elements from e-waste.[16–32] In this study, we report that a 2D form of the earth-abundant silicon—siloxene nanosheets (denoted as SiNSs)—has exceptionally high gold extraction capability, and can work under mild conditions and in a relatively wide working pH range. When extracting gold from a 10 ppm Au solution at 45 °C and 60 °C, SiNSs achieved extraction capacities of 1336.6 mg g^{-1} and 1507.9 mg g^{-1}, respectively. Moreover, they can extract gold at extremely low concentrations, down to a few ppb, with high selectivity. During the extraction, SiNSs reduced more than 99.99% of the gold ions to metallic gold, eliminating the need for desorption, concentration, and precipitation treatments typically required after adsorption. This reductive recovery mechanism exhibited lower activation energy than chemisorption processes. Additionally, the selective extraction of high-value metals, such as Au and Cu, can be prioritized while minimizing the adsorption of other, lower-value elements commonly found in real electronic waste. Finally, we demonstrate an efficient flow-through process for gold extraction using SiNS membranes. Our findings indicate that SiNSs, as an abundant and non-toxic two-dimensional material on Earth, exhibit remarkable potential for applications in electronic waste recycling and the reduction of precious metals.

Results and discussion

Highly efficient gold extraction by SiNSs

SiNSs were obtained by exfoliating commercially mass-produced $CaSi_2$ (pre-treated with NaOH) using 1 M hydrochloric acid (HCl) *via* our previously developed protocol.[21] This method can produce partially oxidized 2D silicon (Fig. S1, Table S1 and Note S1, ESI†), with high surface area (reaching 281.38 m^2 g^{-1}, with the pore size of clearly a few nanometres, as shown in Fig. S2, ESI†),[21] and abundant amounts of the reductive Si–H bonds, which is known as a mild reducing reagent and has been proved to be an excellent platform for loading metals.[16–18,20,33,34] The extraction process is shown in Fig. 1.

The dried SiNSs were directly added to the Au-ion-containing solution (as shown in Fig. 2a). Because the hydrometallurgy process is a flexible, low-cost, and sustainable method for e-waste recycling, and $[AuCl_4]^-$ is the most common gold complex seen in such process and many gold-containing wastewater systems, we first chose $HAuCl_4$ solutions prepared in different concentrations to examine the gold extraction capacity of SiNSs (Fig. 2b). Consistent with high performance at high Au concentrations for many materials, the extraction capacity of SiNSs increased overall with increasing Au concentration. Specifically, 1 g of SiNSs could extract 532.6, 554.3, 666.4, 587.5, 551.0, and 665.8 mg of gold from gold solutions with concentrations of 0.5, 1, 5, 10, 50, and 100 ppm, respectively (reaction time: 24 h, pH = 2, at room temperature (25 °C)). This extraction performance is superior to that of most nanoporous Au-capturing materials at the same concentration levels (Table S2, ESI†). More importantly, SiNSs could successfully extract gold from solutions with gold concentrations below 10 ppb (Fig. S3, ESI† and Fig. 4). Although we could not quantify the extraction performance of SiNSs at this concentration due to the detection limit of the quantification method, we observed significant gold extraction. Given that freshwater typically contains less than 10 ppb of gold, SiNSs could potentially be effective for gold recovery in such environments.

In addition to concentration, the extraction capacity of SiNSs varies with the pH of the solution, a common phenomenon

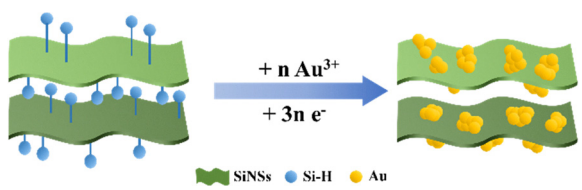

Fig. 1 Schematic illustration of the reductive extraction of Au ions with SiNSs.

This journal is © The Royal Society of Chemistry 2025

Published on 25 2025. Downloaded on 08.08.2025 20:24:34.

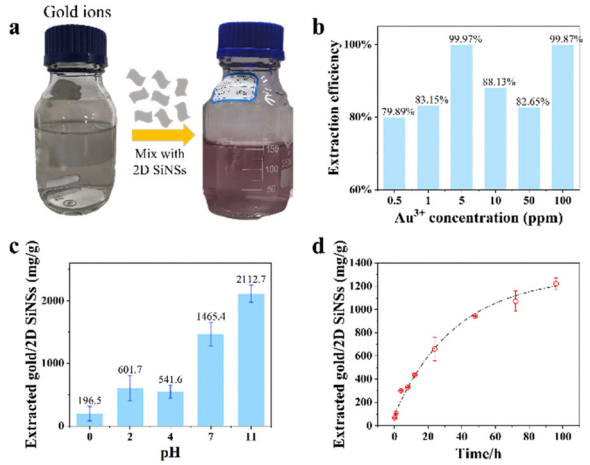

Fig. 2 (a) A photograph of the extraction process using SiNSs. After being mixed with SiNSs for 24 h, observable color emerged in the gold ion solution (10 ppm), indicative of the formation of metallic Au. (b) Relationship between extraction capacity and gold concentration (24 h). (c) Relationship between extraction efficiency and solution pH (10 ppm). (d) Variation in extraction efficiency with time (10 ppm). All experiments at 10 ppm were conducted at 25 °C using the same amount of SiNSs. Error bars in this figure represent the standard deviation.

observed for gold extraction.[2,9,11,26–29,35–38] The extraction capacity of SiNSs in Fig. 2c shows a monotonic increase over the pH. Under neutral or alkaline conditions with a pH $\geq$ 7, the extraction capacity is maximized, with 1 g of SiNSs capable of extracting over 1400 mg of gold. This is in stark contrast from the traditional systems in which high pH usually results in the hindrance of adsorption or reduction.[39–42] This is likely due to the gradual etching of SiNSs in the mildly alkaline environment, which exposes the Si–H bonds within the SiNSs, thereby enhancing their extraction performance. However, considering that electronic waste leachate in industrial processes is typically acidic, it is more appropriate to select a pH range of 1 to 4 for the SiNS extraction environment. Nevertheless, in principle, by increasing the amount of SiNSs, it is still possible to extract approximately 99% of gold from a 10 ppm gold solution at the whole pH range of 0–11.

Additionally, we studied the gold extraction over time (as shown in Fig. 2d). The extracted gold amount increased monotonically without any induction period. Basically after 24 hours, 1 g of SiNSs could extract over 700 mg of gold from a 10 ppm gold solution, and the number could reach over 1200 mg of gold after 96 hours (pH = 2, at room temperature (25 °C)). This result indicates that SiNSs have a decent extraction rate and a high total capacity for gold extraction. Interestingly, even within minutes, the gold solution with added SiNSs changed from transparent to purplish-red (the color of gold nanoparticles), suggesting the instant reductive recovery of Au and strong reducing ability of SiNSs (Video S1, ESI†). The extraction rate within the initial 60 minutes was significant (Fig. S5 and Note S2, ESI†).

Mechanism study of SiNSs' gold extraction behavior

To understand the high gold extraction behavior of SiNSs, we started with the characterization of SiNSs after gold extraction. After placing SiNSs in the gold solution for 24 hours, we observed gold nanoparticles of varying sizes on the surface of SiNSs (as shown in Fig. 3a). Energy dispersive X-ray spectrometer (EDS) analysis of the same location confirmed the presence of gold element. X-ray photoelectron spectroscopy (XPS) analysis also supported this finding (Fig. 3b), indicating that the particles were zero-valent metallic gold with negligible amount of oxidized Au ions. Most novel gold adsorbents in the literature primarily rely on physical and chemical adsorption, although some exceptions exhibit a certain degree of reductive adsorption. As a result, these adsorbents extract a mixture of ionic gold and metallic gold, necessitating energy- and cost-intensive post-treatment processes, such as elution and precipitation, to desorb and reduce ionic gold.[5,6,11,36,43,44] In contrast, SiNSs can reduce gold ions to metallic gold without additional post-treatment, thereby providing a further advantage for gold extraction using SiNSs. To investigate the kinetic principles of this redox reaction, this study evaluated the gold extraction capability of 2D SiNSs under different temperature (T) conditions (reaction time: 24 h, pH = 2). Since the gold extraction capability of the 2D SiNSs in this reaction is directly governed by the redox reaction rate, a plot of extraction capability *versus* temperature was constructed (as shown in Fig. 3c). The results reveal that the extraction capacity of SiNSs increases with increasing temperature, reaching 1507.9 mg g^{-1} at 60 °C. The data were subsequently fitted to the Arrhenius equation.

$$k = A e^{-\frac{E_a}{k_B T}}$$

Here, k is the reaction rate constant; A is the pre-exponential factor (also known as the frequency factor); E_a represents the activation energy barrier; k_B is the Boltzmann constant; and T is the thermodynamic temperature.

Based on the results, we roughly calculated that the reaction has an apparent energy barrier of 0.17 $\pm$ 0.02 eV, which is lower than the activation energy observed in most common chemisorption processes (0.21–4.3 eV).[45] Consequently, the 2D SiNSs demonstrate excellent extraction performance and rapid extraction rates even in low-concentration gold standard solutions.

Moreover, increasing the temperature can further enhance the extraction capability of the 2D SiNSs. For example, at ambient temperatures of 45 °C and 60 °C, with a gold concentration of only 10 ppm, the observed extraction capacities reached 1336.6 mg g^{-1} and 1507.9 mg g^{-1}, respectively.

Additionally, we characterized the SiNSs before and after the reaction using Fourier transform infrared (FTIR) spectroscopy (Fig. 3d). The SiNSs exhibited distinct Si–H characteristic peaks before the reaction. However, after the reaction, the intensity of these Si–H peaks decreased or even disappeared, and the signal ratio of Si–O–Si/Si–H significantly increased.

In another set of experiments, we tested the gold extraction capacity of commercial nano-silicon powder (with an average diameter of below 100 nm) and found it to be less than 50 mg g^{-1} (Fig. S6, ESI†). FTIR characterization results also indicated that this commercial nano-silicon powder had almost no Si–H characteristic peaks (Fig. S7, ESI†). This result further suggests that the occurrence of a redox reaction between the gold ions and SiNSs was responsible for the high extraction capability.

Published on 25 2025. Downloaded on 08.08.2025 20:24:34.

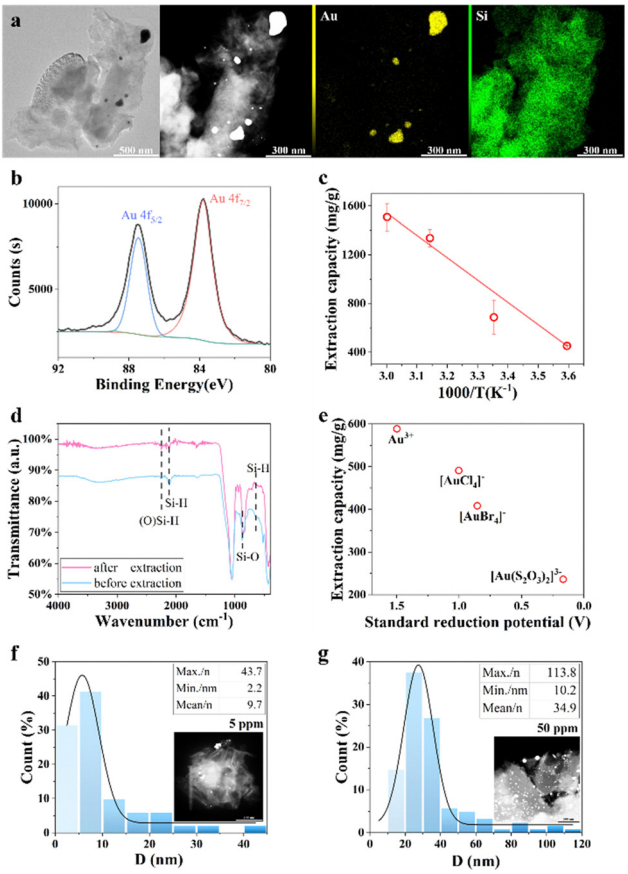

Fig. 3 (a) TEM images and EDS analysis of SiNSs after gold extraction. From left to right: bright field, dark field, EDX image of Au, and EDS image of Si. (b) XPS analysis of the Au 4f spectrum of gold nanoparticles on the surface of SiNSs. The black curve represents the raw data. (c) Variation in gold extraction performance of SiNSs with temperature. The red straight line represents the data fitting curve used to calculate the reaction energy barrier. (d) FTIR spectra of SiNSs before extraction (blue line) and after extraction (red line). (e) Extraction capacity of SiNSs for gold complexes with different reduction potentials. TEM images and particle size analysis of gold nanoparticles extracted from SiNSs at 5 ppm (f) and 50 ppm (g) gold concentrations.

To further demonstrate the redox nature of the extraction process, we measured the extraction capacity of SiNSs for gold ions with different reduction potentials (E_0) (Fig. 3e). An evident correlation curve was established using solutions containing Au^{3+}, $[AuCl_4]^-$, $[AuBr_4]^-$, and $[Au(S_2O_3)_2]^{3-}$, supporting our conclusion that the redox reaction between gold ions and SiNSs governs the observed behavior.

Based on the above experimental results, we propose the following mechanism for the high gold extraction capacity of SiNSs. Firstly, the extraction is driven by the concentration difference (ΔC) of the ion between the solution and the extracting material:[46] $\Delta C = C_{sol}^{Au\ ion} - C_{SiNSs}^{Au\ ion}$. Once gold ions approach SiNSs, they rapidly convert to metallic Au, leaving an extremely low concentration of gold ions ($C_{SiNSs}^{Au\ ion}$) on the SiNSs, thereby maintaining a high ΔC throughout the extraction process. This enables SiNSs to overcome rapid equilibrium at low concentrations and exhibit excellent extraction capacity even at ppb levels. Secondly, the large specific surface area of SiNSs facilitates the reductive extraction of gold ions, while the abundant Si–H groups on the SiNSs provide sufficient reducing capacity for recovering gold ions to metallic Au. Such reductive loading on 2D silicon structures has also been previously observed with Cu and Pd ions.[16,21,47]

Interestingly, while investigating the effect of different initial concentrations of gold solutions on the extraction capacity of SiNSs, we observed some variance, and higher concentrations did not necessarily enhance the extraction performance of SiNSs. As shown in Fig. 2b, a slight decline in extraction performance was observed when the concentration increased from 5 ppm to 50 ppm. To explore the underlying mechanism of this phenomenon, we collected SiNSs after extraction at gold ion concentrations of both 5 ppm and 50 ppm, and characterized them using transmission electron microscopy (TEM) and EDS, as shown in Fig. 3f and g. From these observations, we identified a significant difference in the particle sizes of the extracted gold nanoparticles between the two concentrations. The average particle size of Au extracted at 5 ppm was noticeably smaller than that of Au extracted at 50 ppm. The large particle size indicates that excessive Au was further reduced at the surface of Au particles initially formed. An increase in the Au particle size may result in lower capacity for adsorption of Au species and hinder the contact with hydride of the SiNSs, thus slowing down the Au ion reduction.[48]

When the Au concentration is significantly larger (100 ppm), the huge concentration difference (ΔC) again dominates to drive the high extraction capacity. The bottom line is that SiNSs are well suited for applications involving the treatment of Au at such low-concentration levels, which may align well with some real industrial electronic wastewater treatment scenarios in which the valuable metals contained are scarce.

Efficient gold recovery *via* continuous flow-through systems

To better align with industrial aqueous solution treatment scenarios and demonstrate the potential of SiNSs for industrial gold extraction from wastewater or leachate, we adopted an alternative approach. In this approach, SiNSs were fabricated into membranes with a mass of approximately 30 mg and a diameter of 4.5 cm, enabling low-concentration gold solutions to continuously flow through the SiNS membranes (as shown in Fig. 4a). Fig. 4b shows the extraction performance of the SiNS membrane during the filtration of 7 L of 100 ppb gold solution. We observed that the extraction efficiency remained almost constant above 99% up to 3 L, after which it decreased to 95–96%. Simultaneously, the gradual accumulation of gold nanoparticles between the SiNS nanosheets began to block water flow (as shown in Fig. 4c), and the permeability of the membrane gradually declined. However, this typical reduction in the performance, common in adsorption-based membrane separation processes,[49,50] can be mitigated by using membranes in series.

Concurrently, we conducted a control experiment comparing gold concentrations before and after passing through the pristine cellulose membrane. As shown in Table S3 (ESI†), no significant change in the concentration of gold was observed,

 This journal is © The Royal Society of Chemistry 2025

Published on 25 2025. Downloaded on 08.08.2025 20:24:34.

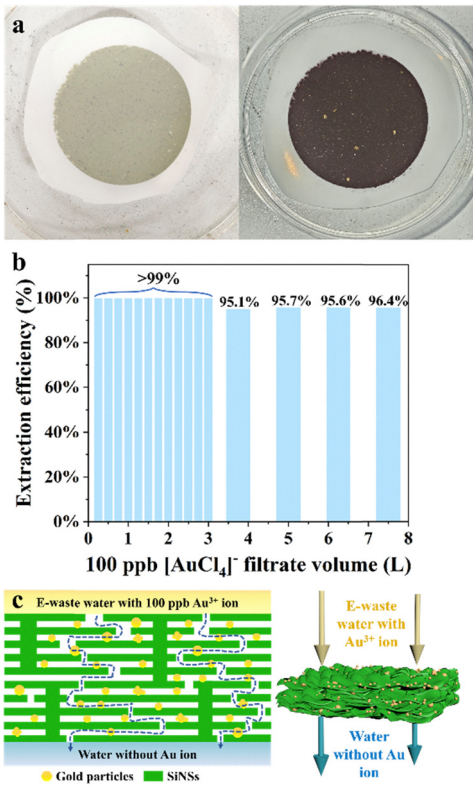

Fig. 4 (a) Images showing the SiNSs films before extraction (left) and after extraction (right), respectively. (b) As the volume of 100 ppb Au solution filtered increases, there was no significant decrease in the extraction efficiency of the SiNSs film. (c) Sectional (left) and 3D (right) schematic diagrams illustrating the extraction of low-concentration gold solutions using SiNSs films.

confirming that the cellulose membrane exerts negligible influence on Au^{3+} ion extraction.

Real-world gold extraction

To conduct the final feasibility evaluation of this technology for e-waste recycling, authentic waste computer central processing units (CPUs) were processed *via* standard hydrometallurgical methods to prepare representative e-waste leachates. The leachate contained gold (Au) alongside a significant amount of copper (Cu), minor amounts of nickel (Ni), zinc (Zn), palladium (Pd) (a coexisting noble metal), and trace levels of aluminum (Al), iron (Fe), and chromium (Cr). The primary metal species and their concentrations are summarized in Table 1.

Gold extraction was subsequently performed using two approaches: mixing SiNSs with the e-waste leachate and filtering the leachate through a SiNS membrane using a continuous flow-through extraction device. The gold extraction capacities and efficiencies observed in both methods are presented in Fig. 5a and b, respectively. Both extraction methods demonstrated the high selectivity of SiNSs for gold ions, with the e-waste leachates yielding Au recovery rates of 98% and 92%, respectively. Although approximately 50% of palladium (Pd), aluminum (Al), and iron (Fe) were co-extracted in the mixing method, their significantly lower abundance in the feedstock

Table 1 Metal elements and their concentrations in authentic waste CPU leachate

Metallic elements	Concentration/ppm
Cu	24.78
Au	9.73
Ni	3.21
Zn	2.00
Pd	0.57
Al	0.03
Fe	0.02
Cr	0.01

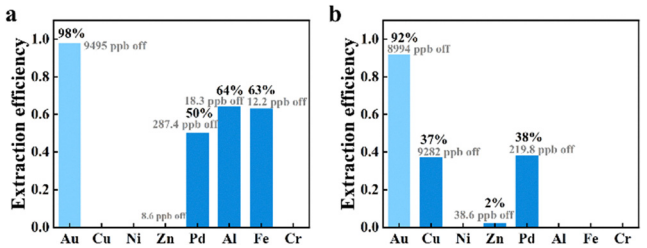

Fig. 5 (a) The extraction efficiency of each element by SiNSs when they are directly mixed with the e-waste leaching solution. (b) Extraction efficiency of constituent elements from e-waste leachate processed in the continuous flow-through extraction system.

resulted in minimal absolute quantities recovered (<5% of total extracted metal mass). In the faster flow-through method, only the highly valuable metals Cu and Pd exhibited some extraction efficiency (below 40%), which is to be expected since they can be reduced by SiNSs. In the continuous-flow method, the significantly shorter contact time between metal ions and SiNSs compared to batch mixing leads to less extraction efficiencies of the low-value Al and Fe ions, which are prone to be captured through traditional adsorption in the prolonged batch mixing process. Meanwhile, unlike the batch system where sufficient duration enables sequential displacement reactions (*e.g.*, metallic Cu gradually replacing Au(III) ions according to the metal activity series), the continuous-flow approach results in a slight decrease in selectivity for Au while demonstrating an increase in selectivity for Cu. Such metals are also in principle easy to be removed through standard acid treatment in gold purification industries.

Final isolation of metallic gold piece

In the final step, we used a 2 M NaOH solution to remove the SiNSs and the cellulose acetate membrane substrate, and the precipitate was analyzed using TEM and EDS (as shown in Fig. 6a). It was found that under alkaline conditions, the gold nanoparticles spontaneously aggregated into larger gold particles, and even some with the largest size were visible to the naked eye (as shown in Fig. 6b). The purity of the Au in the EDS analysis was over 99%, and the SiNSs were completely removed, with the impurity peak signal in EDS analysis being less than 1%. To further accelerate the aggregation process, the Au obtained from the alkaline treatment was placed in a tube furnace and heated at 1000 °C. Within 60 minutes, the Au

Published on 25 2025. Downloaded on 08.08.2025 20:24:34.

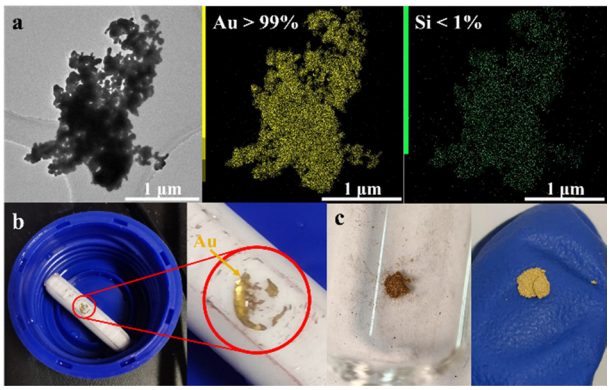

Fig. 6 (a) TEM image and EDS analysis results of Au recovered on SiNSs after NaOH treatment, with Au content >99%. (b) Spontaneous aggregation of metallic Au on a stirring magnet. (c) Macroscopic metallic gold piece formed before (left) and after (right) a short calcination step at 1000 °C.

particles had fused into visible gold chunks (as shown in Fig. 6c). Unlike other extraction methods, this process requires only a brief heating treatment for the Au, making it an efficient and energy-saving method for recovering Au from wastewater.

From an economic perspective, the entire recovery process is feasible. If we define 50% extraction efficiency as the end-of-life for the SiNS membrane,[51] it is estimated that 1 g of SiNSs can extract approximately 0.67 g of gold from wastewater containing 100 ppb of gold ions. Besides, the production cost of SiNSs is less than 0.07 dollars per g (as estimated in Note S3, ESI†).

The price of gold is around 99.13 dollars per g as of April 2025, which results in a very rough estimated return of approximately 949 times. Although this estimation, based on material costs, does not account for other associated expenses, our feasible chemical processes exhibited minimal energy requirements, involving no need for advanced equipment and highly specialized training for operation. Combined with the high gold extraction capacity, precise selectivity, and scalability of SiNSs, there is significant potential for the commercial recovery of gold from electronic waste, although continuous efforts are required for further optimization and scaling up. Future study might explore gold extraction scenarios at even lower concentration levels using SiNSs, such as from seawater, due to the low extraction concentration limit and the fact that the reductive extraction process does not consume other reactants.

Experimental

Preparation of SiNSs

A typical synthesis of SiNSs started from the etching of $CaSi_2$: NaOH which was dissolved in water to form a solution with a concentration of 5 M. The mixture of 2.0 g of $CaSi_2$ and 200 mL of NaOH solution was kept stirred at room temperature for 14 hours. After the reaction, the solid from the mixture, named $CaSi_2$–NaOH, was collected by centrifugation, washed with water, and dried under vacuum sequentially. 1.0 g of $CaSi_2$–NaOH was added to 100 mL of pre-diluted hydrochloric acid (1 M) in a round-bottom flask. The mixture was stirred at 25 °C for 4.5 days in N_2. Then, the solvent was removed after centrifugation. The remaining solid was dried under vacuum after being washed with ethanol twice.

Extraction efficiency of SiNSs

We prepared gold solutions by diluting the stock solution of gold ions ($HAuCl_4$) with deionized water to obtain final gold concentrations of 0.5, 1, 5, 10, 50, and 100 ppm. The pH of the mixtures was adjusted to 2 by adding HCl or NaOH. Subsequently, SiNSs were added to the solution for mixing. In this situation, the weight ratio of Au ions to SiNSs was maintained at 1 : 1.5. At each time point, the mixture was filtered using a 13 mm PES syringe filter with a pore size of 0.22 μm. The filtrates were then analyzed using inductively coupled plasma optical emission spectroscopy (ICP-OES) and inductively coupled plasma mass spectrometry (ICP-MS) to determine the extraction efficiency, R (%), which was calculated as

$$R = \frac{C_0 - C_e}{C_0} \times 100\%$$

where C_0 is the initial concentration of Au (ppm) and C_e is the final concentration in the filtrate (ppm).

Extraction capacity of SiNSs

We selected extraction durations ranging from 15 minutes to 96 hours, with the mixtures stirred at a speed of 500 rpm. To rule out the effect of pH, we followed the same procedure as above, uniformly adjusting to pH = 2 by adding HCl or NaOH. To ensure reproducibility, all measurements were repeated at least three times. For detailed information on gold extraction using commercial silicon nanoparticles, see Fig. S7 (ESI†). For the extraction of gold from different gold complexes by SiNSs, we followed a similar procedure to that for extracting gold from $HAuCl_4$ solution. To study the effect of temperature on gold adsorption performance, extraction experiments were conducted at 5, 25, 45, and 60 °C. 3 mg of SiNSs were added to 400 mL of the gold solution with a final gold concentration of 10 ppm. Due to the high extraction capacity under conditions exceeding 48 h and temperatures above 45 °C, the volume of the initial 10 ppm Au ion solution was increased to 800 mL for scaled testing. For SiNSs' gold extraction from different gold complexes, we followed a similar procedure to that for gold extraction from $HAuCl_4$ solutions. To distinguish between the diluted $HAuCl_4$ solution and the $KAuCl_4$ solution stabilized with abundant HCl, the former is labelled as Au^{3+} and the latter as $AuCl_4^-$ in this experiment. Note that Au^{3+} is unstable and it is difficult to acquire its pure solution; the standard reduction potential labelled thus does not represent the actual value for this solution which still has an abundant amount of stable $AuCl_4^-$, but it helps to supplement the trend showing the correlation between the extraction performance *vs.* reducibility of the ions. Unless otherwise stated, all experiments were conducted at room temperature (25 °C), and the initial concentration was 10 ppm in all cases.

This journal is © The Royal Society of Chemistry 2025

Published on 25 2025. Downloaded on 08.08.2025 20:24:34.

We measured extraction efficiency for 10 ppm solutions at pH of 0, 2, 4, 7, and 11. The pH was adjusted by adding 1 M of HCl and 1 M of NaOH solutions. 3 mg of SiNSs were added to 400 mL of the gold solution with the final gold concentration of 10 ppm. Due to the high extraction capacity at pH $\geq$ 7, the total amount of the initial 10 ppm gold ion solution was increased to 800 mL. After stirring at a speed of 500 rpm for 24 hours, the mixtures were filtered and analysed using ICP-OES to determine the extraction capacity Q_e (mg g^{-1}). It was calculated as follows:

$$Q_e = \frac{(C_0 - C_e) \times V}{m}$$

where C_0 is the initial concentration of Au (ppm), C_e is the final concentration in the filtrate (ppm), V is the volume of the suspension used (L), and m is the mass of the dried SiNSs (g).

Flow-through extraction

30 mg of SiNSs were dispersed in 30 mL of deionized water under thorough mixing at room temperature. The homogeneous suspension was subsequently poured into a Brinell funnel equipped with a cellulose acetate membrane (0.22 μm pore size, diameter: 4.5 cm). Vacuum filtration was applied to remove all deionized water, resulting in a uniformly distributed SiNSs film. The performance of the obtained film was evaluated using a 100 ppb Au solution. Following filtration of every 250 mL aliquot, the gold extraction efficiency was determined *via* inductively coupled plasma mass spectrometry (ICP-MS) analysis.

Real-world gold extraction

The CPU waste solution is obtained from discarded computer components. To extract gold from CPUs, they are first soaked in an 8 M NaOH solution for 48 hours to remove the protective coating on the electronic surfaces. The CPUs are then thoroughly rinsed and immersed in 40 mL of concentrated nitric acid for 48 hours. After washing, the CPUs are placed in 50 mL of aqua regia for 48 hours. Undissolved materials are filtered out, and NaOH is added to the filtrate to achieve pH = 2. This results in a leachate with a concentration of 170 $\pm$ 50 ppm, and the solution is then diluted to a suitable concentration for later use. The leachate is filtered through a SiNSs membrane at room temperature to extract gold. The amount of extracted gold is evaluated using at least three samples following the aforementioned procedure. The elemental composition of the filtrate is analyzed *via* inductively coupled plasma mass spectrometry (ICP-MS). All experiments are conducted at room temperature (25 °C).

Characterization

TEM images and EDX mappings were performed on a JEOL JEM F200 (200 kV) transmission electron microscope. Fourier-transform infrared (FTIR) spectroscopy was performed using a Bruker Alpha FTIR spectrometer fitted with a universal attenuated total reflectance sampling accessory. X-ray photoelectron spectroscopy (XPS) was obtained using a Thermo Scientific K-Alpha Scanning ESCA Microprobe instrument (physical electronics) equipped with an Al Kα X-ray source ($h\nu$ = 1486.6 eV) and binding energies referenced to C 1s (284.8 eV). The metal content of different samples was measured using an inductively coupled plasma optical emission spectrometer (ICP-OES) (Thermo Fisher iCAP PRO), and an inductively coupled plasma mass spectrometer (ICP-MS) (Agilent 7850). The O and H content of the material was analysed using an oxygen, nitrogen and hydrogen analyser (HORIBA EMGA-830).

Conclusions

In this work, focusing on gold (Au)—the most valuable element in electronic components, solution-phase synthesized SiNSs were demonstrated to have exceptional Au extraction capacity (as high as >1500 mg of Au per gram of SiNSs) in low-concentration simulated Au-containing wastewater/leachate (10 ppm). Systematic tests were conducted to evaluate the Au extraction performance of SiNSs under varying conditions (time, temperature, and pH) using the most common Au-bearing simulated solutions. The redox extraction mechanism was distinct from the common adsorption mechanism for most nanomaterials, elucidated through pre- and post-extraction characterization studies of SiNSs, analysis of extraction performance over different gold-containing ions, and the low activation energy barrier. Furthermore, authentic e-waste leachate was prepared from discarded central processing units (CPUs), from which Au ions were successfully recovered using SiNSs. To better simulate industrial-scale e-waste treatment scenarios, a continuous-flow extraction device was developed, enabling Au recovery from simulated Au-containing solutions *via* SiNS membrane filtration. This device achieved >99% Au removal efficiency from ultradilute Au solutions (100 ppb) and maintained >95% efficiency after processing >7 L of wastewater, while also exhibiting robust performance in treating CPU-derived e-waste leachate. Finally, metallic gold precipitates were successfully recovered from the simulated wastewater through NaOH-mediated dissolution of SiNSs, yielding macroscopically visible gold pieces.

Author contributions

W. S. and D. K. conceived and designed the experiments. D. K. performed all sample preparation and characterization. C. X. assisted in the analysis of the experimental mechanism and the construction of the continuous-flow extraction device. S. W. assisted with the FTIR characterization experiments. C. Z. and Y. D. contributed to the metallic gold sintering experiments. D. Y. provided advice on the comprehensive strategy and manuscript writing. D. K. and W. S. wrote the manuscript. All authors reviewed and commented on the final manuscript.

Conflicts of interest

There are no conflicts to declare.

Published on 25 2025. Downloaded on 08.08.2025 20:24:34.

Data availability

All data generated or analyzed during this study are presented in this published article and its ESI.† Original raw data can be provided from the authors upon reasonable request.

Acknowledgements

This work was supported by the National Key R&D Program of China (Grant No. 2021YFF0502000), the National Natural Science Foundation of China (Grant No. 52372233), and the China Postdoctoral Science Foundation (No. 2024M762820).

Notes and references

1 M. D. Rao, K. K. Singh, C. A. Morrison and J. B. Love, *RSC Adv.*, 2020, **10**, 4300–4309.
2 P. Thaveemas, V. Phouthavong, T. Hagio, D. Dechtrirat, L. Chuenchom, S. Nijpanich, N. Chanlek, J.-H. Park and R. Ichino, *Sep. Purif. Technol.*, 2024, **343**, 127113.
3 J. Cui and L. Zhang, *J. Hazard. Mater.*, 2008, **158**, 228–256.
4 F. Yang, Z. Yan, J. Zhao, S. Miao, D. Wang and P. Yang, *J. Mater. Chem. A*, 2020, **8**, 3438–3449.
5 D. T. Sun, N. Gasilova, S. Yang, E. Oveisi and W. L. Queen, *J. Am. Chem. Soc.*, 2018, **140**, 16697–16703.
6 T. T. Ma, R. Zhao, Z. N. Li, X. F. Jing, M. Faheem, J. Song, Y. Y. Tian, X. J. Lv, Q. H. Shu and G. S. Zhu, *ACS Appl. Mater. Interfaces*, 2020, **12**, 30474–30482.
7 W. Q. Zhan, Y. Yuan, B. Q. Yang, F. F. Jia and S. X. Song, *Chem. Eng. J.*, 2020, **394**, 124866.
8 F. Q. Liu, S. J. You, Z. Y. Wang and Y. B. Liu, *ACS ES&T Eng.*, 2021, **1**, 1342–1350.
9 Z. C. Liu, M. Frasconi, J. Y. Lei, Z. J. Brown, Z. X. Zhu, D. Cao, J. Iehl, G. L. Liu, A. C. Fahrenbach, Y. Y. Botros, O. K. Farha, J. T. Hupp, C. A. Mirkin and J. F. Stoddart, *Nat. Commun.*, 2013, **4**, 1855.
10 L. M. M. Kinsman, B. T. Ngwenya, C. A. Morrison and J. B. Love, *Nat. Commun.*, 2021, **12**, 6258.
11 Y. Hong, D. Thirion, S. Subramanian, M. Yoo, H. Choi, H. Y. Kim, J. F. Stoddart and C. T. Yavuz, *Proc. Natl. Acad. Sci. U. S. A.*, 2020, **117**, 16174–16180.
12 Y. Wu, Q. Fang, X. Yi, G. Liu and R.-W. Li, *Prog. Nat. Sci.: Mater. Int.*, 2017, **27**, 514–519.
13 A. F. M. Nogueira, A. R. F. Carreira, S. J. R. Vargas, H. Passos, N. Schaeffer and J. A. P. Coutinho, *Sep. Purif. Technol.*, 2023, **316**, 123797.
14 F. Kubota, R. Kono, W. Yoshida, M. Sharaf, S. D. Kolev and M. Goto, *Sep. Purif. Technol.*, 2019, **214**, 156–161.
15 E. D. Doidge, L. M. M. Kinsman, Y. Ji, I. Carson, A. J. Duffy, I. A. Kordas, E. Shao, P. A. Tasker, B. T. Ngwenya, C. A. Morrison and J. B. Love, *ACS Sustainable Chem. Eng.*, 2019, **7**, 15019–15029.
16 C. Qian, W. Sun, D. L. H. Hung, C. Qiu, M. Makaremi, S. G. H. Kumar, L. Wan, M. Ghoussoub, T. E. Wood, M. Xia, A. A. Tountas, Y. F. Li, L. Wang, Y. Dong, I. Gourevich, C. V. Singh and G. A. Ozin, *Nat. Catal.*, 2019, **2**, 46–54.
17 X. Yan, W. Sun, L. Fan, P. N. Duchesne, W. Wang, C. Kuebel, D. Wang, S. G. H. Kumar, Y. F. Li, A. Tavasoli, T. E. Wood, D. L. H. Hung, L. Wan, L. Wang, R. Song, J. Guo, I. Gourevich, F. M. Ali, J. Lu, R. Li, B. D. Hatton and G. A. Ozin, *Nat. Commun.*, 2019, **10**, 2608.
18 S. Wang, K. Feng, D. Zhang, D. Yang, M. Xiao, C. Zhang, L. He, B. Yan, G. A. Ozin and W. Sun, *Adv. Sci.*, 2022, **9**, 2104972.
19 X. Yan, W. Sun, W. Wang, P. N. Duchesne, X. Deng, J. He, C. Kuebel, R. Li, D. Yang and G. A. Ozin, *Small*, 2020, **16**, 2001435.
20 S. Wang, C. Wang, W. Pan, W. Sun and D. Yang, *Sol. RRL*, 2021, **5**, 2000392.
21 Y. Su, S. Wang, L. Ji, C. Zhang, H. Cai, H. Zhang and W. Sun, *Nanoscale*, 2022, **15**, 154–161.
22 X. Liu, L. Ma, P.-W. Han, Z. Yang, Z. Li, J. Yan, Y. Wang and S. Ye, *ACS Sustainable Chem. Eng.*, 2022, **10**, 15305–15318.
23 J. Luo, X. Luo, M. Xie, H.-Z. Li, H. Duan, H.-G. Zhou, R.-J. Wei, G.-H. Ning and D. Li, *Nat. Commun.*, 2022, **13**, 7771.
24 L. Zhang, J.-Q. Fan, Q.-Q. Zheng, S.-J. Xiao, C.-R. Zhang, S.-M. Yi, X. Liu, W. Jiang, Q.-G. Tan, R.-P. Liang and J.-D. Qiu, *Chem. Eng. J.*, 2023, **454**, 140212.
25 H. Zhou, W. Zhao, S. Zhang, X. An, H. Lan, H. Liu and J. Qu, *Resour., Conserv. Recycl.*, 2023, **198**, 107165.
26 Y.-R. Chen, X.-Y. Fan, H.-F. Wei, L. Liao, Y. Hu, Y. Lu, X. Wang, Y. Li and W.-R. Cui, *Sep. Purif. Technol.*, 2024, **347**, 127521.
27 K. Yang, K. G. Nikolaev, X. Li, I. Erofeev, U. M. Mirsaidov, V. G. Kravets, A. N. Grigorenko, X. Qiu, S. Zhang, K. S. Novoselov and D. V. Andreeva, *Adv. Sci.*, 2025, **12**, 2408533.
28 K. Yang, K. G. Nikolaev, X. Li, A. Ivanov, J. H. Bong, I. Erofeev, U. M. Mirsaidov, V. G. Kravets, A. N. Grigorenko, S. Zhang, X. Qiu, K. S. Novoselov and D. V. Andreeva, *Proc. Natl. Acad. Sci. U. S. A.*, 2024, **121**, e2414449121.
29 P. Bhadane, D. Menon, P. Goyal, M. R. A. Kiapi, B. K. Satpathy, A. Lanza, I. Mikulska, R. Scatena, S. Michalik, P. Mahato, M. Asgari, X. Chen, S. Chakraborty, A. Mishra, I. Lynch, D. Fairen-Jimenez and S. K. Misra, *Sep. Purif. Technol.*, 2025, **360**, 130946.
30 C. Zhang, G. Zhao, D. Zhang, S. Wang and W. Sun, *Inf. Funct. Mater.*, 2024, **1**, 108–123.
31 D. Zhang, C. Zhang, S. Wang and W. Sun, *J. Zhejiang Univ., Sci., A*, 2024, **25**, 877–888.
32 M. Li, R. Ramachandran, T. Sakthivel, F. Wang and Z.-X. Xu, *Chem. Eng. J.*, 2021, **421**, 129728.
33 X. Pei, D. Zhang, R. Tang, S. Wang, C. Zhang, W. Yuan and W. Sun, *Nanoscale*, 2024, **16**, 12411–12419.
34 Y. Nagai, *Org. Prep. Proced. Int.*, 1980, **12**, 13–48.
35 C. Wang, G. Lin, J. L. Zhao, S. X. Wang, L. B. Zhang, Y. H. Xi, X. T. Li and Y. Ying, *Chem. Eng. J.*, 2020, **380**, 122511.
36 T. S. Nguyen, Y. R. Hong, N. A. Dogan and C. T. Yavuz, *Chem. Mater.*, 2020, **32**, 5343–5349.
37 W. Q. Liu, L. O. Jones, H. Wu, C. L. Stern, R. A. Sponenburg, G. C. Schatz and J. F. Stoddart, *J. Am. Chem. Soc.*, 2021, **143**, 1984–1992.

 This journal is © The Royal Society of Chemistry 2025

38 Q. M. Yang, J. Cao, F. C. Yang, Y. C. Liu, M. M. Chen, R. R. Qin, L. X. Chen and P. Yang, *Chem. Eng. J.*, 2021, **416**, 129066.
39 B. J. Morrow, E. Matijevic and D. V. Goia, *J. Colloid Interface Sci.*, 2009, **335**, 62–69.
40 J. Zhao, C. Wang, S. Wang, L. Zhang and B. Zhang, *J. Cleaner Prod.*, 2019, **236**, 140212.
41 C. Kojima, Y. Umeda, A. Harada and K. Kono, *Colloids Surf., B*, 2010, **81**, 648–651.
42 Q. Shen, Q. Min, J. Shi, L. Jiang, W. Hou and J.-J. Zhu, *Ultrason. Sonochem.*, 2011, **18**, 231–237.
43 P. Chen, Y. M. Liang, B. Q. Yang, F. F. Jia and S. X. Song, *ACS Sustainable Chem. Eng.*, 2020, **8**, 3673–3680.
44 C. Wu, X. Y. Zhu, Z. Wang, J. Yang, Y. S. Li and J. L. Gu, *Ind. Eng. Chem. Res.*, 2017, **56**, 13975–13982.
45 D. Liping, S. Yingying, S. Hua, W. Xinting and Z. Xiaobin, *J. Hazard. Mater.*, 2007, **143**, 220–225.
46 L. Feng, Y. Y. Qiu, Q. H. Guo, Z. J. Chen, J. S. W. Seale, K. He, H. Wu, Y. N. Feng, O. K. Farha, R. D. Astumian and J. F. Stoddart, *Science*, 2021, **374**, 1215–1221.
47 M. Ohashi, R. Yaokawa, Y. Takatani and H. Nakano, *ChemNanoMat*, 2017, **3**, 534–537.
48 B. G. Ershov, E. V. Abkhalimov, R. D. Solovov and V. I. Roldughin, *Phys. Chem. Chem. Phys.*, 2016, **18**, 13459–13466.
49 M. Peydayesh and R. Mezzenga, *Nat. Commun.*, 2021, **12**, 3248.
50 S. J. Ling, Z. Qin, W. W. Huang, S. F. Cao, D. L. Kaplan and M. J. Buehler, *Sci. Adv.*, 2017, **3**, e1601939.
51 F. Li, J. Zhu, P. Sun, M. Zhang, Z. Li, D. Xu, X. Gong, X. Zou, A. K. Geim, Y. Su and H.-M. Cheng, *Nat. Commun.*, 2022, **13**, 4472.

Published on 25 2025. Downloaded on 08.08.2025 20:24:34.